# MECHANICAL SURFACE TREATMENTS ON THE HIGH-STRENGTH WROUGHT MAGNESIUM ALLOY AZ80

2005/02

P. Zhang1, J. Lindemann1, A. Kiefer2 and C. Leyens1

1 Lehrstuhl Metallkunde und Werkstofftechnik, BTU-Cottbus, Postfach 101344, D-03013, Cottbus, Germany
2 OSK Kiefer GmbH, A. d. unt. Kreuzstück 10, D-07381, Oppurg, Germany

## ABSTRACT
The influence of shot peening and roller burnishing on the fatigue performance of high-strength wrought magnesium alloy AZ80 has been investigated. Shot peening was conducted on smooth specimens by using different peening mediums (glass beads, Zirblast B30 and Zr-$CeO_2$ ($ZrO_2$ spherical particles stabilized by $CeO_2$)) and different Almen intensities (0.04 – 0.40 mmN). Roller burnishing was performed under different rolling forces from 50 – 400 N. The results show that both shot peening and roller burnishing improve the fatigue life of AZ80 significantly. The improvement in fatigue strength by shot peening is in the range of 60-75% at optimum conditions for different peening mediums. Compared to shot peening, roller burnishing can more effectively enhance the fatigue strength of AZ80, the improvement in fatigue strength by roller burnishing is about 110% at the optimum condition.

## SUBJECT INDEX
Fatigue, Wrought magnesium alloy, AZ80, Mechanical surface treatments

## INTRODUCTION
High-strength wrought magnesium alloys are considered as potential candidates for application as suspension parts in future automobiles (Aune 1992, Friedrich 2000). For this application, good high cycle fatigue (HCF) performance must be achieved. It is well known that mechanical surface treatments such as shot peening, roller burnishing and deep rolling enhance the fatigue performance of structural metallic materials (Gregory 2003, Lang 2003, Lindemann 2003). Recently, the work by Wagner and Hilpert (Wagner 1999, Hilpert 2000) has shown that the fatigue life of high-strength magnesium alloys can be improved by shot peening and roller burnishing. In order to apply these techniques for practical magnesium applications, further indepth investigations are yet to be performed.

In the present work, the influence of shot peening and roller burnishing on fatigue performance of the high-strength wrought magnesium alloy AZ80 has been investigated. In order to establish optimum conditions with regard to fatigue performance, shot peening and roller burnishing were performed using a wide variation in Almen intensity and rolling force, respectively.

## EXPERIMENTAL
The high-strength wrought magnesium alloy AZ80 (nominal composition in wt.%: 8Al, 0.5Zn, 0.2Mn, balance: Mg) used in the present work was produced by Otto Fuchs Metallwerke, Meinerzhagen, Germany. The alloy was forged to a rectangular bar with

a cross section of 60 mm × 11 mm. After forging, the alloy exhibits a single $\alpha$-phase structure with an average grain size of 30 μm. Texture measurement results show that the basal planes are oriented predominantly parallel to the longitudinal–transversal (L–T) plane. The material was tested in the as received condition without any heat-treatment.

Specimens were machined with the load axis parallel to longitudinal direction of the rectangular bars. Tensile tests were performed on threaded cylindrical specimens having gage lengths of 20 mm at initial strain rates of $8.3 \times 10^{-4}$ $s^{-1}$. Tensile test results are shown in Table 1.

**Table 1:** Tensile results on the wrought magnesium alloy AZ80

| Material | Testing direction | $\sigma_{0.2}$ (MPa) | UTS (MPa) | EL (%) | RA (%) |
|---|---|---|---|---|---|
| AZ80 | L | 226 | 337 | 18.2 | 25.2 |

For fatigue testing, hour-glass shaped round specimens (6 mm gage diameter) were used. After machining, a layer with a thickness of about 200 μm was removed from the surface of the specimens by electrolytical polishing (EP) in order to avoid any influence of machining on the fatigue results.

Shot peening (SP) was performed with an injector type machine using different peening mediums such as glass beads, Zirblast B30 and Zr-$CeO_2$ ($ZrO_2$ spherical particles stabilized with $CeO_2$). Details of the peening medium are listed in Table 2. The distance between nozzle tip and specimen surface was about 80 mm. To determine the best HCF response, specimens were shot-peened by glass, Zirshot B30 and Zr-$CeO_2$ to full coverage using Almen intensities in the range of 0.04 –0.4 mmN. Roller burnishing (RB) was performed using a one-roll hydraulic system with 6 mm hard-metal ball operating on a conventional lathe. The spindle speed was 36 $min^{-1}$; rolling forces were varied between 50-400 N.

**Table 2:** Parameters of the peening mediums

| Peening medium | Composition (wt%) | Diameter (μm) | Hardness | Density ($g \cdot cm^{-3}$) |
|---|---|---|---|---|
| Glass beads | 70% $SiO_2$, 10% CaO, 15% $Na_2O$+ $K_2O$, 5% MgO | 300-400 | 47 (HRC) | 2.5 |
| B30 | 60-70% $ZrO_2$, 28-33%$SiO_2$, >10%$Al_2O_3$ | 425-600 | 600-800 (HV1) | 3.8 |
| Zr-$CeO_2$ | 80-90% $ZrO_2$, 10-20%$CeO_2$ | 600-800 | 1224 (HV3) | 6 |

The surface properties of specimens after SP and RB were determined by roughness measurements through profilometry, measurements of the microhardness–depth profiles and residual stress measurements by means of the incremental hole drilling method (Schwarz 1992).

Fatigue tests were performed under rotating beam loading (R = -1) at a frequency of about 100 Hz in air.

**RESULTS AND DISCUSSION**

The influence of SP and RB on the resulting surface roughness values is plotted in Fig. 1. It can be seen that SP leads to a marked increase in surface roughness (Fig. 1a). For glass and Zirblast B30 peened specimens severe surface defects such as overlaps and microcracks are observed when the Almen intensity is above 0.20 mmN. Interestingly, specimens shot-peened by Zr-$CeO_2$ yield the lowest value of surface roughness, and severe surface defects are hardly seen even at the highest Almen intensity of 0.4 mmN.

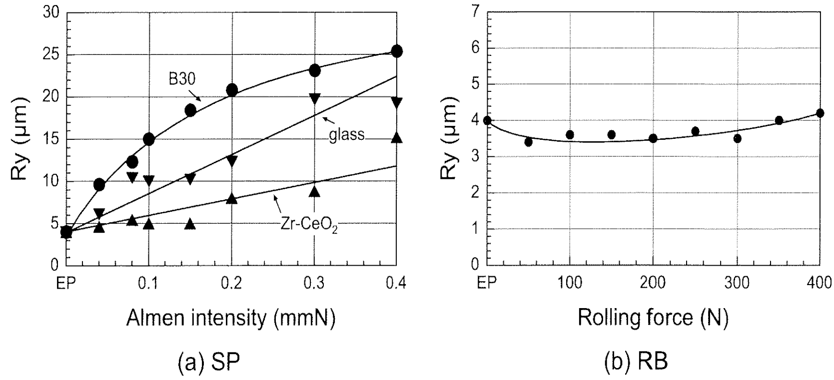


**Figure 1:** Surface roughness profile of AZ80 after SP and RB.

In contrast to SP, RB results in a relatively smoother surface (Fig. 1b). The surface roughness after RB firstly decreases with increasing rolling force, then slightly increases as the rolling force is higher than 350N. Smoother surfaces after RB can markedly improve the resistance of fatigue crack initiation and hence enhance the fatigue life.

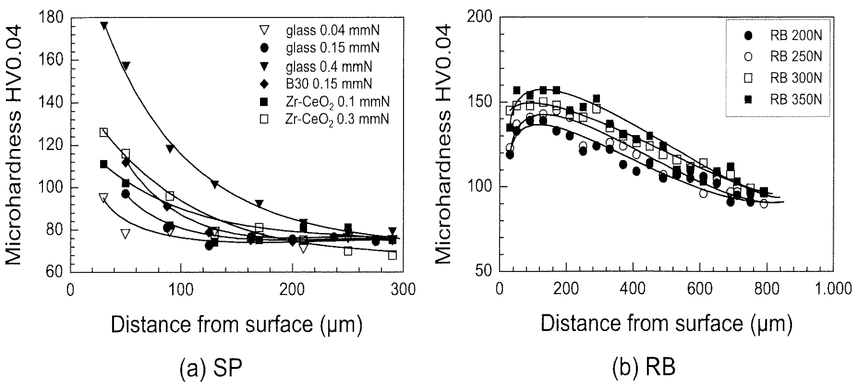


**Figure 2:** Microhardness-depth profile after SP and RB.

Figure 2 shows microhardness–depth profiles after SP and RB. Owing to shot peening induced plastic deformation, there is a pronounced increase in microhardness in the near-surface region (Fig. 2a). Increasing the Almen intensity from 0.04 to 0.4 mmN leads to greater depths of plastic deformation. The thickness of plastic deformation layer resulting from SP can be estimated to be about 50-200 μm for the different Almen intensities from 0.04-0.4 mmN. As opposed to SP, much greater depths of plastic deformation can be induced by RB, and the thickness of the deformation layer after RB can be estimated to be about 700-800 μm from the microhardness profiles in Fig. 2b.

Figure 3 shows the residual stress distribution in AZ80 after SP and RB. It can be seen that both SP and RB induced compressive residual stresses. The maximum compressive residual stresses resulting from SP are about 45-100 MPa for the different Almen intensities ranging from 0.04-0.4 mmN. In contrast to SP, RB induced higher compressive residual stresses, e.g. the maximum compressive residual stress of 340 MPa is located at the surface if the specimen is roller burnished with a roller force of 200 N.

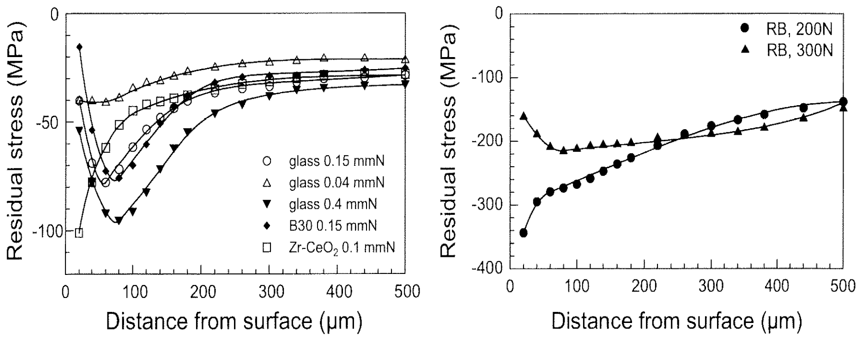


(a) SP (b) RB

**Figure 3:** Residual stress–depth profile after SP and RB.

The effect of Almen intensity on fatigue life at the stress amplitude of 175 MPa is shown in Fig. 4. A marked over-peening effect is found in the specimens shot-peened by glass and Zirblast B30, i.e. with increase in the Almen intensity, the fatigue life first dramatically increases, then drops drastically. The highest life improvements of roughly two orders of magnitude are obtained at the optimum condition with Almen intensity of 0.15 mmN. In contrast, the over-peening effect in the specimens shot-peened by Zr-$CeO_2$ is less pronounced. This indicates the importance of surface roughness on fatigue performance after SP. Run-outs ($10^7$ cycles) are found already at intermediate Almen intensities of about 0.08-0.10 mmN. With further increase in Almen intensity, there is only a slight decrease in fatigue life.

The over-peening effect of magnesium alloys was observed earlier by Wagner (1999). Significant life improvement was obtained on the high-strength AZ80 only at a very low intensity of 0.05 mmN. In contrast, the optimum condition for SP in the present work moves to higher intensities and the process window becomes much larger. These differences in fatigue behaviour after SP are possibly associated with the different microstructures in the two materials (Zhang 2005).

The stress–life (S-N) curves at the optimum condition for SP are shown in Fig. 5. Compared to the reference specimens (EP), SP improves the fatigue life at all stress amplitudes. The fatigue limit increases from 100 to 160, 160 and 175 MPa for the specimens shot-peened by glass, Zirblast B30 and Zr-$CeO_2$, respectively. The corresponding improvements in fatigue limit are about 60, 60, and 75%.

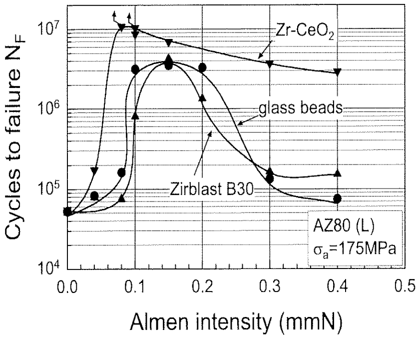


**Figure 4:** Fatigue life vs. Almen intensity at the stress amplitude of $\sigma_a$=175 MPa.

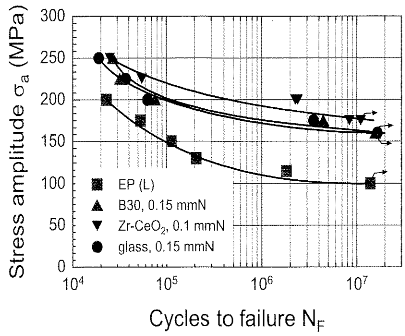


**Figure 5:** S-N curves of AZ80 after optimum shot peening conditions (rotating beam loading in air).

The effect of rolling force on the fatigue life at a constant stress amplitude of $\sigma_a$=225 MPa is illustrated in Fig. 6. Similar to the over-peening effect found in SP, the magnesium alloy sensitively responses to rolling force, i.e. the fatigue life first increases with the increase in rolling force, then gradually decreases as the rolling force further increases. From Fig. 6, it can be seen that the maximum improvement in fatigue life is more than two orders of magnitude at rolling forces between 200 – 300 N. The decrease in fatigue life for F > 300 N results from the lower residual compressive stresses at the surface (Fig 3b). Therefore, we take the rolling force of 200 N as the optimum condition.

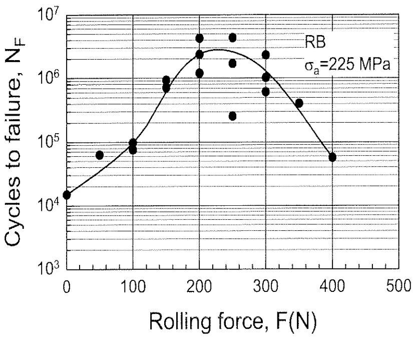


**Figure 6:** Fatigue life ($\sigma_a$= 225 MPa) vs. rolling force.

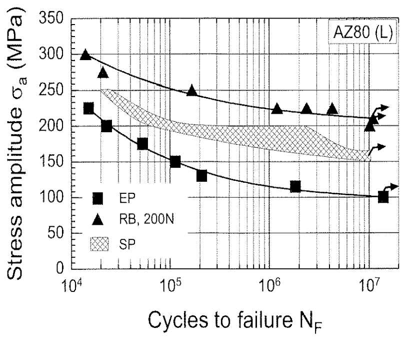


**Figure 7:** S-N curve of AZ80 after optimum RB conditions. The data of S-N curves for AZ80 after SP from Fig. 5 fall into the hatched area.

The S-N curve at the optimum condition (the rolling force of 200 N) for RB is shown in Fig. 7. Compared to the reference specimens (EP), the fatigue life is improved by RB at all stress amplitudes. The fatigue limit increases from 100 to 210 MPa after RB, the improvement is about 110%.

## 4. Conclusions

The investigated AA6110 aluminium alloy shows cyclic hardening in the under-aged condition and cyclic softening in the peak- and over-aged conditions in stress-controlled fatigue tests at room temperature. Deep rolling induced compressive residual stresses and work hardening states into surface regions which result in fatigue lifetime enhancement due to a reduction of the plastic strain amplitude. The effectiveness of deep rolling was governed by the cyclic stability of near-surface work hardening which is known to retard crack initiation. Deep rolling had no beneficial effect on the fatigue life if instability of near-surface work hardening occurred during fatigue test.

## Acknowledgements

The authors would like to express sincere thanks to the German Science Foundation (DFG) under grant no. AL 558/1-2 and to the Faculty of Engineering, Kasetsart University, Thailand, for financial support for Dr. I. Altenberger and Mr. P. Juijerm, respectively.

## References

[1] ASM Metal Handbook: vol. 2, Properties and Selection: Nonferrous Alloys and Special-Purpose Materials, ASM International, Ohio, 1993
[2] I.J. Polmear, Light Alloys, Metallurgy of Light Metals, Halsted Press, London, 1996
[3] W.S. Miller, L. Zhuang, J. Bottema, A.J. Wittebrood, P. De Smet, A. Haszler and A. Vieregge, Mater. Sci. Eng., A 280 (2000) 37
[4] C. Barbosa, J. M. A. Rebello, O. Acselrad, J. Dille and J.-L. Delplancke, Z. Metallkd. 93 (2002) 3
[5] E. Zschech, HTM 51 (1996) 3
[6] L. Wagner, Mater. Sci. Eng. A 263 (1999) 210-216
[7] P. Juijerm, U. Noster, I. Altenberger and B. Scholtes, Mater. Sci. Eng. A 379 (2004) 286
[8] U. Noster, I. Altenberger, B. Scholtes, in: K.U. Kainer (Ed.), Magnesium Alloys and their Applications, Wiley-VCH, Weinheim (2000), p. 274
[9] I. Altenberger, R.K. Nalla, U. Noster, G. Liu, R.O. Ritchie, B. Scholtes, Mat. Wiss. U. Werkstofftech, 34 (2003) 529
[10] R.K. Nalla, I. Altenberger, U. Noster, G.Y. Liu, B. Scholtes, R.O. Ritchie, Mater. Sci. Eng. A 355 (2003) 216
[11] A. Niku-Lari (Ed.), Advances in Surface Treatments, Pergamon Press, Oxford, 1987
[12] B. Scholtes, in: V. Hauk (Ed.), Structural and Residual Stress Analysis by Nondestructive Methods, Elsevier, Amsterdam, 1997, p.590
[13] T. S. Srivatsan and E. J. Coyne, Jr, Int J Fatigue 8 No 4 (1986) p. 201
[14] T. S. Srivatsan, Int J Fatigue 13 No 4 (1991) p. 313
[15] D. Löhe and O. Vöhringer, in G. Totten, M. Howes, and T. Inoue (Ed.), ASM International Handbook of Residual stress and Deformation of Steel, 2002, p.54